

Mechanical, acoustic, and thermal performances of shear thickening fluid-filled rigid polyurethane foam composites: Effects of content of shear thickening fluid and particle size of silica

Ting-Ting Li,^{1,2} Lei Ling,¹ Xiaoxiao Wang,¹ Qian Jiang,^{1,2} Bobo Liu,¹ Jia-Horng Lin,^{1,2,3,4,5,6}
Ching-Wen Lou^{1,6,7,8,9} 

¹Innovation Platform of Intelligent and Energy-Saving Textiles, School of Textile Science and Engineering, Tianjin Polytechnic University, Tianjin 300387, China

²Ministry of Education of Key Laboratory of Advanced Textile Composites, Tianjin Polytechnic University, Tianjin 300387, China

³Laboratory of Fiber Application and Manufacturing, Department of Fiber and Composite Materials, Feng Chia University, Taichung 40724, Taiwan

⁴Department of Fashion Design, Asia University, Taichung 41354, Taiwan

⁵School of Chinese Medicine, China Medical University, Taichung 40402, Taiwan

⁶Ocean College, Minjiang University, Fuzhou 350108, China

⁷College of Textile and Clothing, Qingdao University, Shandong 266071, China

⁸Department of Bioinformatics and Medical Engineering, Asia University, Taichung 41354, Taiwan

⁹Department of Medical Research, China Medical University Hospital, China Medical University, Taichung 40402, Taiwan

Correspondence to: C.-W. Lou (E-mail: cwlou@ctust.edu.tw)

ABSTRACT: Shear thickening fluid (STF) features a rheological property, and rigid polyurethane (PU) foams feature low thermal conductivity and excellent acoustic insulation. In this study, an STF/PU rigid foam composite sandwich structure was designed using different contents (0, 0.5, 1, or 1.5 wt %) of STF that contained 14 nm, 40 nm, or 75 nm silicon dioxide (SiO₂). The effects of STF content and silica size on the cell structure, mechanical performance, acoustic absorption, and thermal performance of the STF/PU foam were explored. The test results show that STF/PU foam exhibited three characteristic acoustic absorption peaks, and the maximum acoustic absorption coefficient reached 0.841. STF addition increased compression, bending strength, and maximum acoustic coefficient, as well as initial mass loss temperature. STF-filled PU foam composites containing 14 nm and 40 nm SiO₂ had a mild rise in thermal insulation. The rigid STF/PU foam composites with a cell structure had the maximum thermal conductivity of 0.22 W m⁻¹ K⁻¹ and sound absorption coefficient of 0.841, which confirm that they are a good candidate for sound-absorbing energy conservation materials. © 2019 Wiley Periodicals, Inc. *J. Appl. Polym. Sci.* **2019**, 136, 47359.

KEYWORDS: foams; mechanical properties; thermal properties; thermogravimetric analysis

Received 1 July 2018; accepted 29 October 2018

DOI: 10.1002/app.47359

INTRODUCTION

Shear thickening fluid (STF) is a newly developed and novel shielding material. It displays flexibility at normal status and becomes highly stiff when impacted.¹ To a certain degree, STF provides comfort and protection, and it is thus the priority choice in applications involving free activity and collisions. STF also features a good cushioning characteristic, making it an ideal material for bulletproof armor.² Noise pollution is an inevitable issue in modern life as it interferes with the quality of sleep, mental status, and work efficiency. In order to attain acoustic absorption, Lin *et al.*³ used a perforation process to provide rigid polyurethane (PU) foam plates with greater load absorption and better acoustic absorption at

medium and high frequencies. Dourbash *et al.*⁴ proposed silica aerogel/rigid polyurethane foam composites and silica aerogel/polyurethane composites. They found that adding silica aerogel to elastomeric PU led to improved acoustic insulation performance. Gama *et al.*⁵ combined crude glycerol and liquefied coffee grounds-derived polyol (POL) to create rigid polyurethane foams with sound absorption efficacy. Increasing the content of POL resulted in a larger cell size and a higher stiffness, which affected the acoustic absorption coefficient of the PU foams. PU foam has a porous cellular structure and good acoustic-absorbing function. The noise-reduction mechanism is as follows: when acoustic energy is transmitted to a foam material, the restrained air inside the cells is

compressed, thereby absorbing the energy waves of the sound waves and preventing them from being reflected.⁶ When STF is incorporated in the preparation of PU foam, the SiO₂ particles narrow the bubbles generated in the foaming process, which strengthens the acoustic absorption performance.⁷

The thermostability of materials indicates how well the material can protect itself from the damage of drastically changing heat, and is thus also a critical characteristic valued in material science.⁸ Therefore, studies on the effects of using various additives on the thermostability of PU foam have become popular in recent years. Michałowski *et al.*⁹ applied polyhedral oligomer silsesquioxane (POSS) modifier to improve the thermostability and flammability of rigid polyurethane foams, and they found that the cellular structure of the foam was dependent on the addition of POSS modifier. Zheng *et al.*¹⁰ used a one-step method to make PU foams using microwave liquefied sugar beet pulp (LSBP) and polymethylene polyphenyl isocyanate, examining the influence of the NCO—/OH— ratio on the mechanical, thermal, and microstructural properties of LSBP/PU foam. Kausar and Siddiq¹¹ compared graphene nanoplatelet (GNP)-reinforced PEI/PU composites and novel poly(ether imide)/polyurethane (PEI/PU)-based nanocomposites, and the measured T_{\max} of PEI/PU/GNP foam 0.1–1 was 479–565 °C. Xu *et al.*¹² measured the thermal stability and flame retardance of rigid PU foam/organoclay nanocomposites using thermogravimetric analysis and cone calorimeter tests. The test results indicated that, compared to pure PU foam, the rigid PU foam/organoclay composites had distinctively enhanced thermal stability and flame retardancy.

STF, composed of dispersion-phase particles and a dispersion medium, is a non-Newtonian fluid with reversibility. The dispersion-phase particles are a natural mineral substance and a chemically synthesized polymer and are in the form of a clay particle, spheroid, disk, or sphere. They are stably dispersed in the solution as polyelectrolytes that are formed by electrostatic interaction, Brownian movement, or graft polymerization. The dispersions include monodispersion, double dispersion, and polydispersion, while the dispersion medium can be water, organics, mineral oil, or a multiple-medium complex.¹³ The modification of PU foam can be done by two methods. One is to add additives during the foaming process. The other is to chemically modify PU foam materials in order to obtain a functional group that has a special performance.¹⁴ PU foam is commonly formed using two agents. The linear-chained dihydric alcohol and a polyhydric alcohol prepolymer undergo a crosslinking reaction with the aid of —NCO. At an appropriate proportion, foaming agent A primarily composed of polyhydric alcohols and foaming agent B containing —NCO have a chemical reaction and release carbon dioxide (bubbles).¹⁵ Notably, rigid PU foam materials have been commonly used as insulating materials¹⁶ due to their good mechanical property, chemical stability, thermal insulation, and acoustic absorption. Rigid PU foam has a honeycomb structure, which easily collects air, and thus has a lower thermal conductivity coefficient¹⁷ and a cell size of one-tenth that of nonfoaming material. An externally applied force exerts elastic deformation on PU foam materials. The restrained air in the interior is compressed, which absorbs part of the impact energy and provides an excellent buffer performance.¹⁸ On average, foam materials

with a high density and small-sized cells have outstanding physical properties. Rigid PU foam material has good cushioning, thermal, insulation, and acoustic absorption properties, though these properties may conflict with others. Therefore, retaining all of the properties of rigid PU foam material has been an emphasis in many studies.¹⁹ In this study, STF is used to increase the mechanical properties, sound absorption efficacy, and thermal insulation of rigid PU foam. The pattern of changes in the porous structure of the rigid PU foam containing STF is analyzed in terms of the particle size of SiO₂ and the content of STF, examining the influence of the two parameters on the aforementioned characteristics.

EXPERIMENTAL

Materials

Poly(ethylene glycol) (PEG; >98%, analytically pure, Tianjin Sanjiang Chemical Technology, Tianjin, China) has high water solubility and organic intermiscibility, making it a good dispersion medium for STF. Absolute ethyl alcohol (Tianjin Sanjiang Chemical Technology, Tianjin, China) is an analytical reagent that serves as cosolvent, facilitating the blending of PEG and silicon dioxide.²⁰ Silicon dioxide (SiO₂, Tianjin Xiangruxin Chemical Technology, Tianjin, China) is used in three sizes of 14 nm, 40 nm, and 75 nm, serving as the dispersion phase of STF. Polyether polyol (Shenzhen Koshengda Trading, Shenzhen, China) has a hydroxyl number of 5 mg KOH/g and a molecular weight of 6000. Isocyanate (Shenzhen Koshengda Trading Shenzhen, China) has a specific weight of 1.25. Low-melting-point poly(ethylene terephthalate) nonwoven fabric (PET; Hsinnyj Nonwoven, Taiwan) has a specification of 200 g/m².

Preparation of STF

In this experiment, STF was prepared using mechanical stirring combined with ultrasonic vibration. First, 15 g of SiO₂ and 85 g of PEG are blended for 2 h at initially 100 rpm and then gradually increased to 900 rpm. During the stirring, a small amount of absolute ethyl alcohol is slowly poured into the mixture so it will blend faster and more uniformly. Then the mixture is processed with ultrasonic vibration for 5 h using an ultrasonic cleaning system, thereby totally distributing the silicon dioxide in the system.²¹ Three batches of STF include 14 nm, 40 nm, or 75 nm SiO₂ separately.

Preparation of Rigid STF/PU Foam Composites

A layer of PET nonwoven fabric is first placed in a 350 mm (length) × 330 mm (width) × 20 mm (thickness) mold. Polyether polyol (100 g), deionized water (1 g), and STF (1 g) are evenly mixed. The mixture and isocyanate (100 g) are blended at a stirring rate of 1000 r/min. When the mixture creates heat, it is swiftly poured into the mold, and more PET nonwoven fabric is placed on it to cover the mixture. It is then sealed to solidify for 25 min.²² A total of nine rigid STF/PU foams are made with contents of STF of 0.5 wt %, 1 wt %, and 1.5 wt % and SiO₂ particle sizes of 14 nm, 40 nm, and 75 nm. The preparation process is shown in Figure 1.

Characterization

Density Test. As specified in ASTM D1622-08, three rigid STF/PU foam composites are taken for each specification. Samples have a

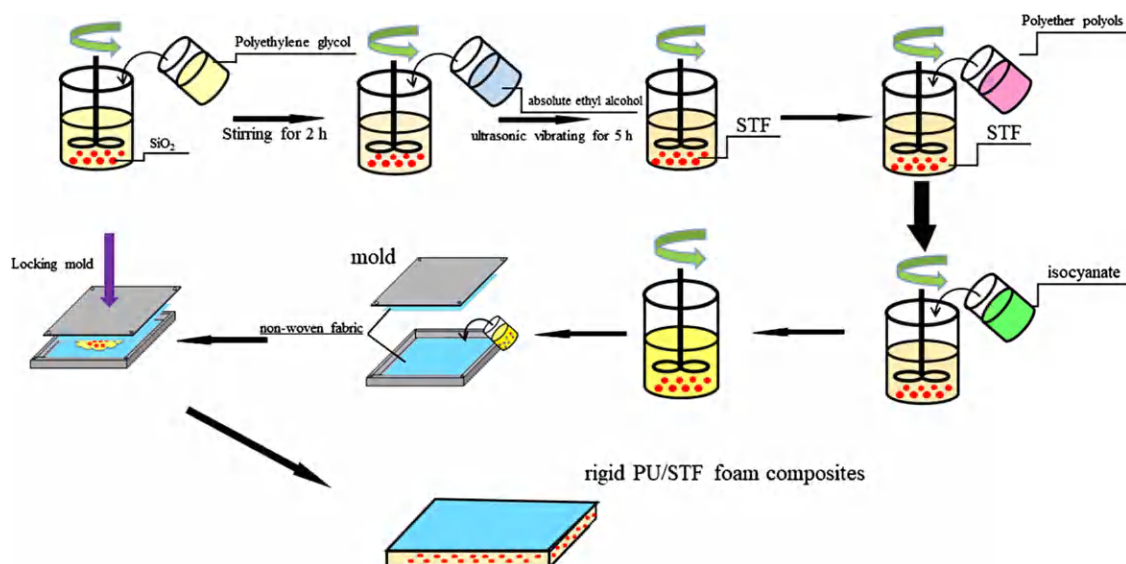


Figure 1. Preparation process of rigid STF/PU foam composites. [Color figure can be viewed at wileyonlinelibrary.com]

size of 50 mm × 50 mm. The thickness is measured using a vernier caliper, which is used to compute the density.

Scanning Electron Microscopy. A scanning electron microscope (SEM; TM1000, Hitachi High-Tech, Tokyo, Japan) is used to observe the transection of the rigid STF/PU foam composites. The cell structure is observed at a magnification of 60 and 120 times. When the images of surface morphology

were analyzed using Image-Pro Plus 6.0 software to obtain the cell diameter, at least two images are calculated for each specification.

Compression Test. As specified in ASTM D1621-16, a universal testing machine (HT-2402, HungTa Instrument, Taiwan) is used to measure the compressive strength of the rigid STF/PU foam composites at a testing speed of 5 mm/min. The specimen size is

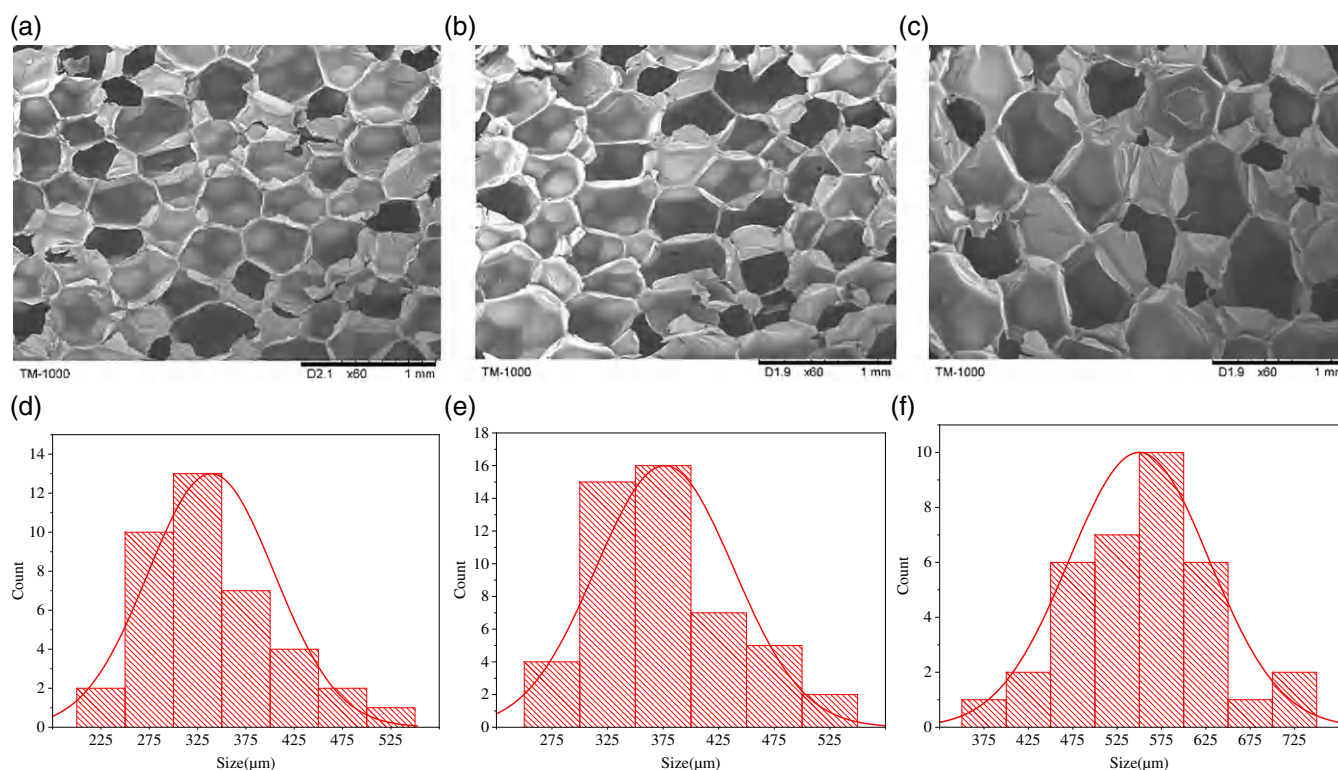


Figure 2. SEM images and cell diameter profiles of rigid STF/PU foam composites made with 1.0 wt % STF containing (a, d) 14 nm, (b, e) 40 nm, and (c, f) 75 nm SiO₂. [Color figure can be viewed at wileyonlinelibrary.com]

Table I. Cell Diameter of Rigid STF/PU Foam Composites as Related to Particle Size of SiO₂

Sample	Average cell diameter (μm)
14 nm SiO ₂ /STF 1 wt %	339.05 ± 64.66
40 nm SiO ₂ /STF 1 wt %	376.46 ± 61.51
75 nm SiO ₂ /STF 1 wt %	549.97 ± 78.20

50 mm × 50 mm × 20 mm. Three samples for each specification are taken for the test.

Bending Test. As specified in ASTM D790-10, a universal testing machine (HT-2402, HungTa Instrument) is used to measure the bending performance of the rigid STF/PU foam composites. The span is 100 mm, and the testing speed is 10 mm/min. Three samples for each specification are taken for the test, and samples have a size of 120 mm × 25 mm × 20 mm.

Thermal Conductivity Measurement. As specified in ASTM C177-13, a thermal conductivity tester (DRX-I-SPB, Xiangtan Huafeng Instrument, Xiangtan, China) is used to measure the thermal conductivity. Three samples for each specification are taken, and samples have a size of 200 mm × 200 mm × 10 mm. The electric furnace temperature is 50 °C.

Acoustic Absorption Measurement. As specified in ASTM E1050-12, a twin-microphone impedance tube (Automotive Research & Testing Center, Taiwan) is used to measure the acoustic absorption coefficient of the rigid STF/PU foam composites.²³ A sample is placed into the impedance tube, and the air layer thickness (the distance between the bottom of the tube and the sample) is 0 cm, 1 cm, and 2 cm. The positions of two microphones are switched after the first measurement, and the second measurement is conducted in order to rectify the difference in the two microphones. The test frequency is between 125 Hz and 4000 Hz, and the test temperature is 24 °C.

Thermogravimetric Analysis. Thermogravimetric analysis (TGA) of the rigid STF/PU foam composites is conducted in nitrogen at a flow velocity of 50 mL/min using a thermogravimetric analyzer (Netzsch TG209F3, Selb, Germany). The heating rate is 10 °C/min, and the heating range is from 50 °C to 800 °C. A fragment of sample of 5 mg is used. The control group is the pure PU foam that does not include STF or SiO₂.

RESULTS AND DISCUSSION

Effect of Content of STF and Particle Size of SiO₂ on Density of Rigid STF/PU Foam Composites

Figure 2 shows the fractured cross-sectional surface of the rigid STF/PU foam composites that are made with 1.0 wt % STF and different particle sizes of SiO₂ of 14 nm, 40 nm, and 75 nm. Table I illustrates the cell diameter of rigid STF/PU foam composites as related to particle size of SiO₂. Figure 3 shows the density of rigid PU foam composites as related to different contents of STF and different particle sizes of SiO₂. The cell size gradually increases as the particle size of SiO₂ increases, as seen in Figure 2(a–f). SiO₂ has a large specific surface area and exerts a high surface tension, so the addition of SiO₂ in the foaming process results in a wider distribution of cell sizes.²⁴ When STF is added, the SiO₂ in the STF as a solid nanoparticle acts as a blowing nucleation agent in the reaction system to produce more and smaller cells, and the cells are pressed against each other to form thicker cell walls. With the same concentration, STF with bigger SiO₂ particles has a lower number of SiO₂ particles, and the viscosity of the PU foam system decreases, which increases the expansion ratio of the resultant foam composites and enlarges the cell diameter of the PU foam.

As shown in Figure 3, the foam density decreases as the content of 14 nm SiO₂ in the STF increases, which is attributed to the reaction of PEG and isocyanate being preferred to the blowing nucleation of the 14 nm–STF additives. For the STF/PU foam composites containing 40 nm and 75 nm SiO₂, the foam density increases to 0.0829 g/mm³ as the STF content increases. This is due to an increase in viscosity caused by the additives in the PU foam. However, the trends in foam density with an increase in

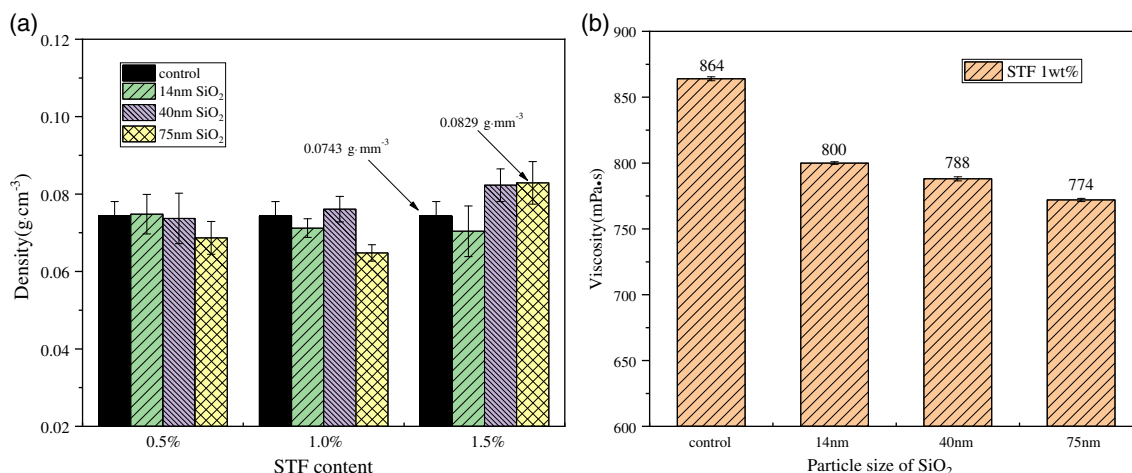


Figure 3. Density of rigid STF/PU foam composites made of different particle sizes of SiO₂ and different contents of STF. [Color figure can be viewed at wileyonlinelibrary.com]

particle size of SiO_2 do not appear stable, as different from cell size indicated in Table I. This is because foam density depends on both the thickness of the cell wall and the size of the cell. With the increase in the particle size of SiO_2 , the bubbles have a relatively smaller volume, which lessens the collision between them, and as such form spherical cells and affect the homogeneity of bubbles and the opened porosity rate.²⁴ Ethylene glycol in STF has a foam reaction with isocyanate, which increases the number of bubbles and decreases the density. However, the STF additive increases the viscosity of the matrix system, reduces the cell size of the foam composites, and increases the foam density. Therefore, in the STF/PU foam, two competing mechanisms affect the density of the foam.

Effect of Content of STF and Particle Size of SiO_2 on Compression Performance of Rigid STF/PU Foam Composites

Figure 4(a) shows the compression performance curve of rigid STF/PU foam composites that are made with 14 nm SiO_2 and different contents of STF. Increasing the content of STF makes the compressive strength first increase and then decrease. Specifically, the composites have the maximum compressive strength when

made with 0.5 wt % STF containing 14 nm SiO_2 . The results indicate that the compression strength of the composites increases to a certain degree with increasing content of STF, but eventually declines when exceeding a certain range of STF. SiO_2 in STF and PEG will generate a granular substance, which is beneficial for compressive strength to a certain degree. An excessive content of STF hampers an even dispersion of STF and causes agglomeration, which creates cells with different diameters. This undermines the morphology of the bubbles in the interior of the foam, and the compressive strength decreases accordingly.²⁵ Figure 4(b,c) shows the compressive strength of the composites that are made with 40 nm and 75 nm SiO_2 as related to different contents of STF. Figure 4(b) shows that with 40 nm SiO_2 , the composites made with 0.5 and 1 wt % STF have greater compressive strength than those made with 1.5 wt % STF. When the content of STF is 1.5 wt %, the composites are composed of SiO_2 at a larger particle size and in a large proportion, which is detrimental to the cell morphology and the compressive strength. By contrast, when the content of STF is 0.5 wt %, the composites are composed of SiO_2 at a larger particle size but in a small proportion, which contributes to a higher compressive strength. Figure 4(c) shows that when the content of STF is 0.5 and

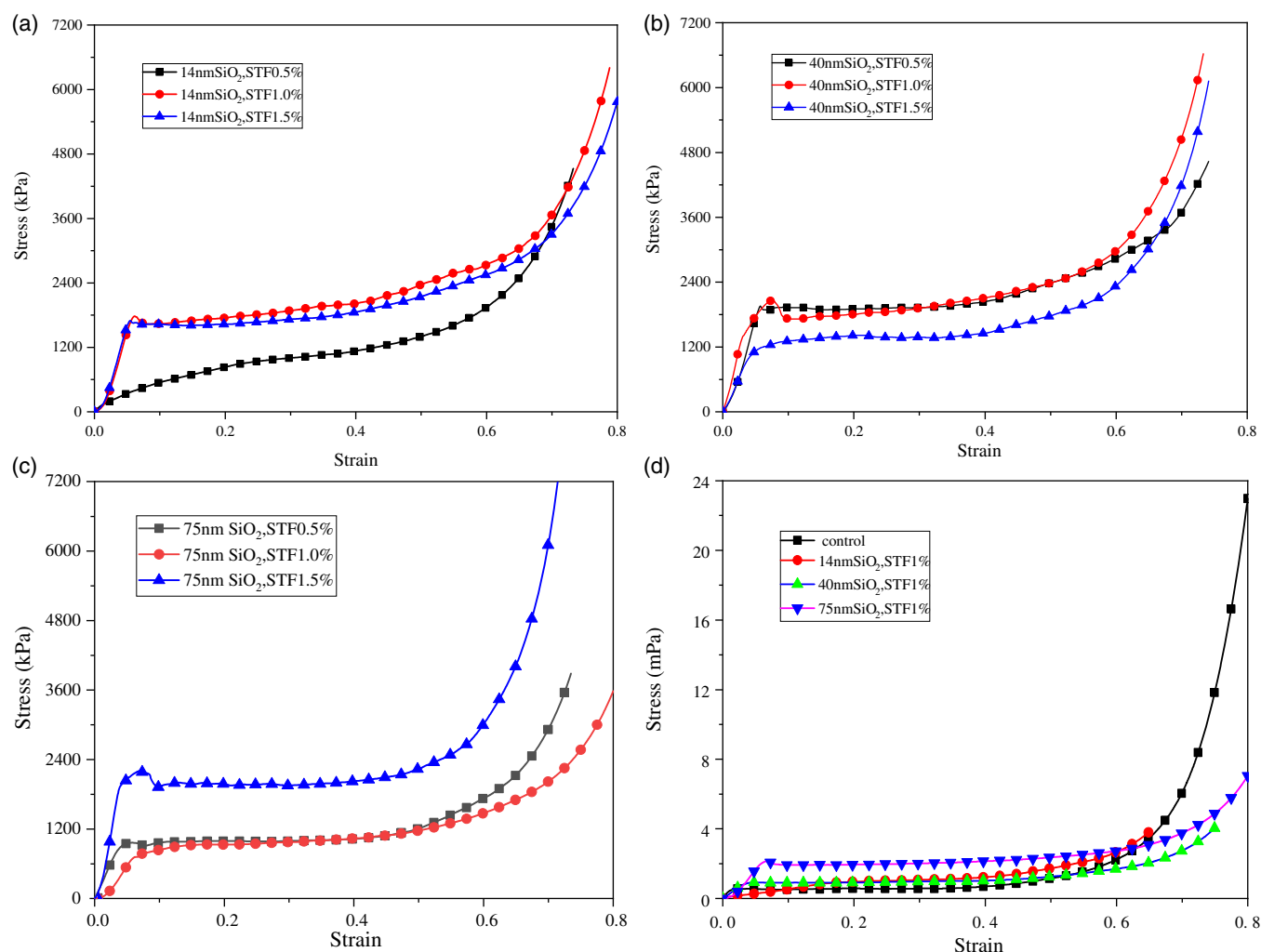


Figure 4. Compressive stress–strain curves of rigid STF/PU foam composites as related to the content of STF and particle size of SiO_2 . [Color figure can be viewed at wileyonlinelibrary.com]

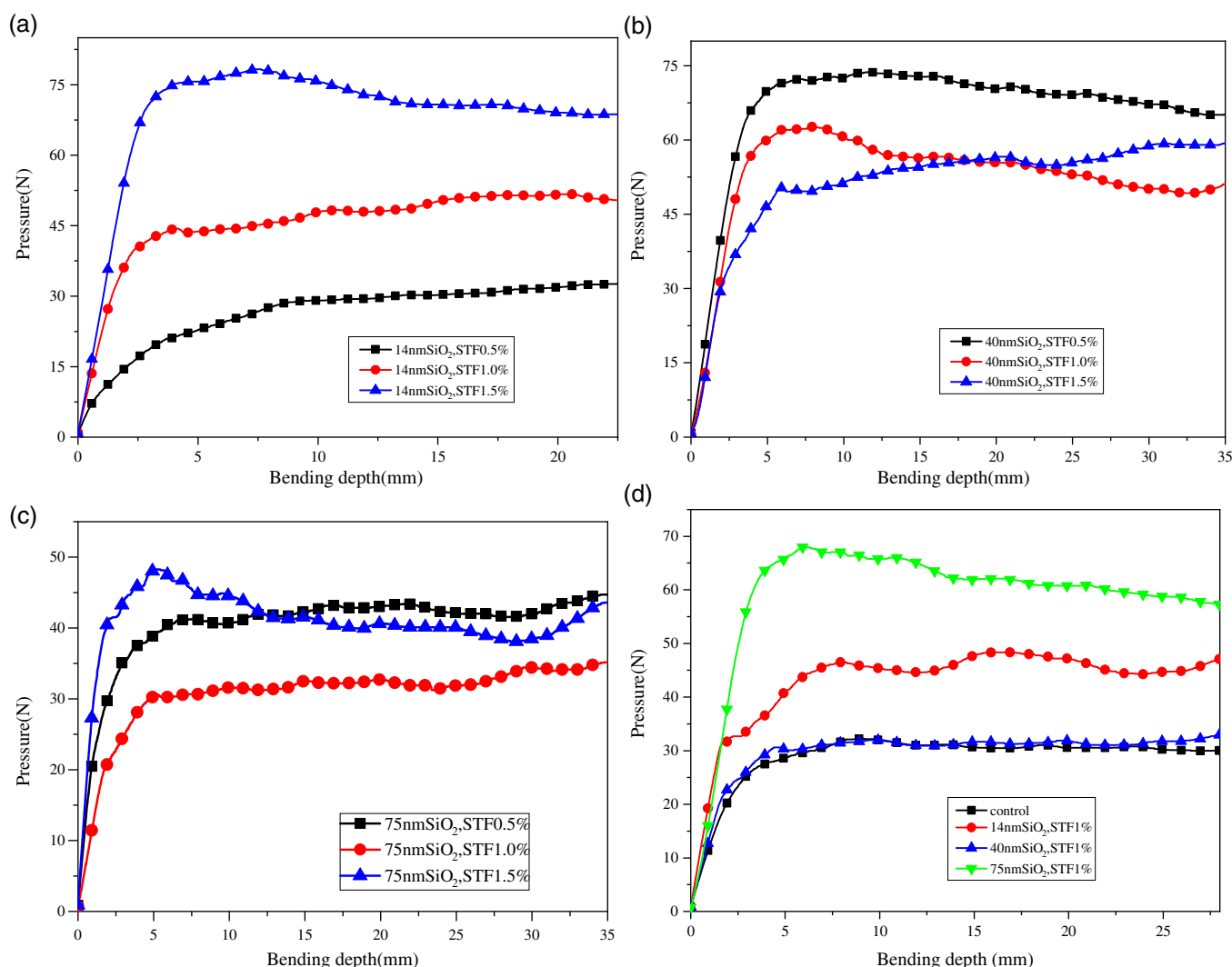


Figure 5. Bending property of rigid STF/PU foam composites as related to the content of STF. [Color figure can be viewed at wileyonlinelibrary.com]

1 wt %, the rigid STF/PU foam composites with 75 nm SiO₂ have a much lower compressive strength than the composites with 40 nm SiO₂. Noticeably, the combination of 75 nm SiO₂ and 1.5 wt % STF inflicts severe damage on the cell morphology, resulting in the maximum compressive strength at this largest proportion. Figure 4 (d) shows the compressive strength of the pure rigid PU foam composites without STF and of the composites made with 1 wt % STF containing 14, 40, and 75 nm SiO₂. The compressive strength of the rigid STF/PU foam composites increases substantially. The larger the SiO₂ particle size, the greater the compressive strength. When an externally applied force is exerted on the composite, SiO₂ nanoparticles take the load, dissipating some accumulated energy caused by stress effects and improving the compressive strength of the composites. SiO₂ is distributed in the polyurethane matrix, which increases the perplexity of soft and hard segments. In addition, hydroxide radicals of SiO₂ and isocyanate groups of polyurethane macromolecules generate chemical bonds or hydrogen bonds, which help in the macromolecular crystallization. To sum up, the presence of SiO₂ accelerates heterogeneous nucleation, which in turn increases the mechanical strength of polyurethane materials.²⁵

Effect of Content of STF and Particle Size of SiO₂ on Bending Property of Rigid STF/PU Foam Composites

Figure 5 shows the bending property curve of the rigid STF/PU foam composites as related to the content of STF and the particle size of SiO₂. Figure 5(a–c) shows that with 14 nm SiO₂, the bending strength of the composites is proportional to the content of STF, which is due to the shear thickening effect of STF. STF consists of alcohols, which makes the addition of STF the equivalent of adding more foaming agent A. This triggers more bubbles during foaming and strengthens the bending property of the composites. Figure 5(c) shows that the lowest and highest bending stress occurs when the composites are made with 40 nm SiO₂ and 1 wt % and 1.5 wt % STF, respectively. Figure 5(b) shows that with a particle size of 75 nm, the bending strength of the composites is inversely proportional to the content of STF. STF contains SiO₂ that reacts with PEG to form particulate matter and strengthen the mechanical properties of the composites. However, excessive STF fails to be dispersed evenly and causes agglomeration and uneven cell size, which adversely affect the cell morphology and the bending property of the composites.²⁶

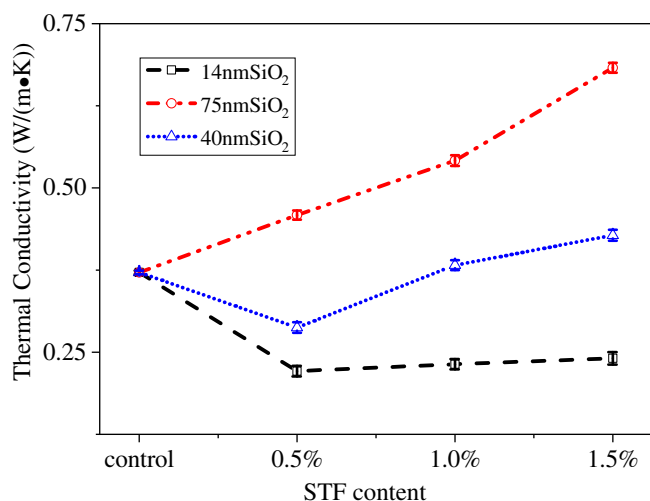


Figure 6. Thermal conductivity of the rigid STF/PU foam composites as related to the content of STF and particle size of SiO₂. [Color figure can be viewed at wileyonlinelibrary.com]

Figure 5(d) shows the bending property curve of pure rigid PU foam without STF and composites made with 1 wt % STF containing 14, 40, and 75 nm SiO₂. The compressive strength of the composites increases as a result of increasing SiO₂ particle size, and then reaches the maximum when the particle size is 75 nm. A greater particle size can strengthen the bending stress of the composites. As nanograde particles, SiO₂ accelerates the formation of polyurethane rigid foam, which causes a smaller cell volume and a greater density. As a result, the composites reach a certain bending strength.^{27,28}

Effect of Content of STF and Particle Size of SiO₂ on Thermal Insulation of Rigid STF/PU Foam Composites

Figure 6 shows the coefficient of thermal conductivity of rigid STF/PU foam composites that are made with different contents of STF that contains SiO₂ at different particle sizes. The pure PU foams without STF have a thermal conductivity of 0.3715 and a low thermal conductivity but a good heat-insulating property. Moreover, with STF containing 14 or 40 nm SiO₂, the composites have a high thermal insulation but a low coefficient of thermal conductivity, which is then proportionally increased with the

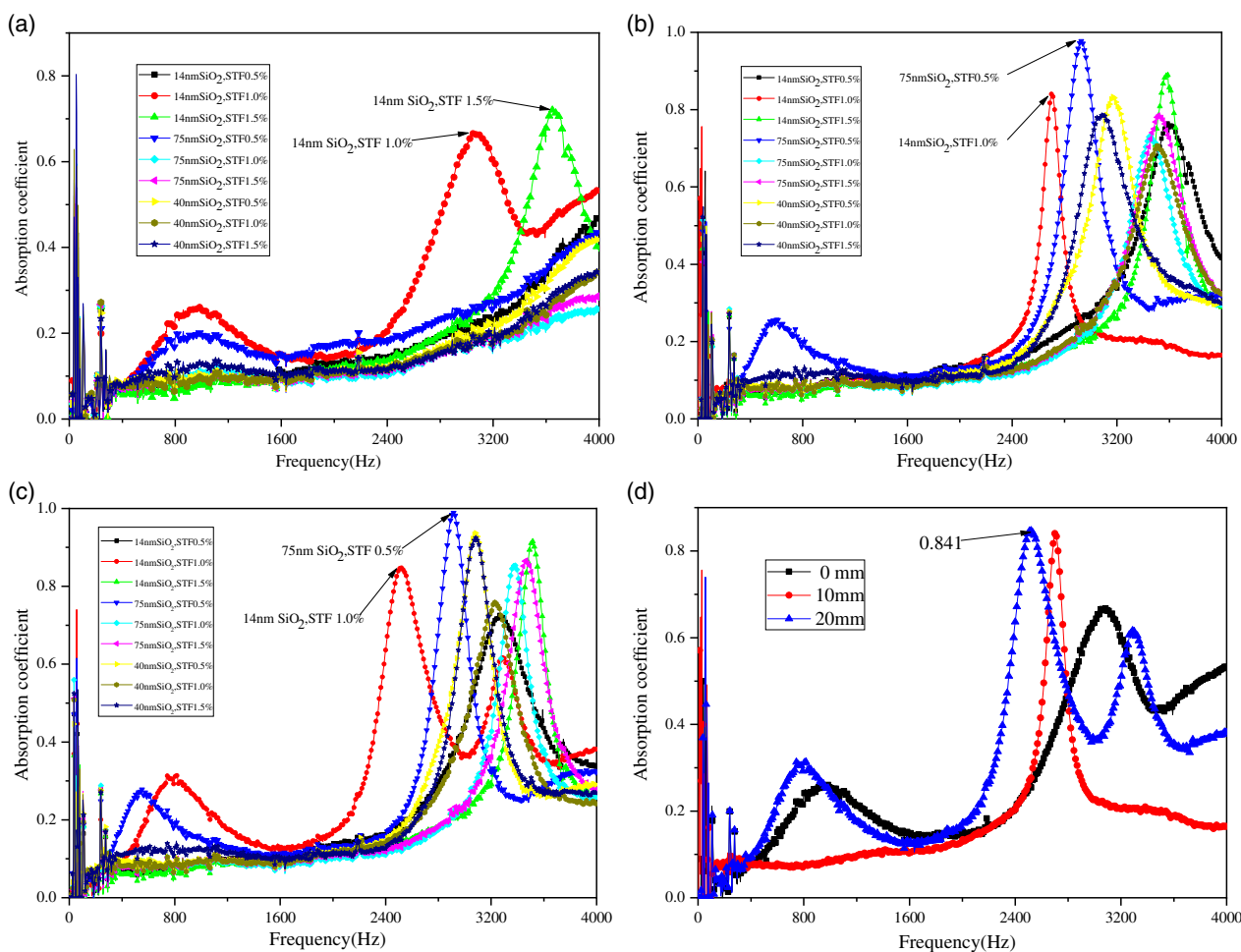


Figure 7. Coefficient of sound absorption of rigid STF/PU foam composites made with different contents of STF as related to the air chamber sizes of (a) 0, (b) 1, and (c) 2 cm. (d) The rigid STF/PU foam composites are made with 1 wt % STF containing 14 nm SiO₂. [Color figure can be viewed at wileyonlinelibrary.com]

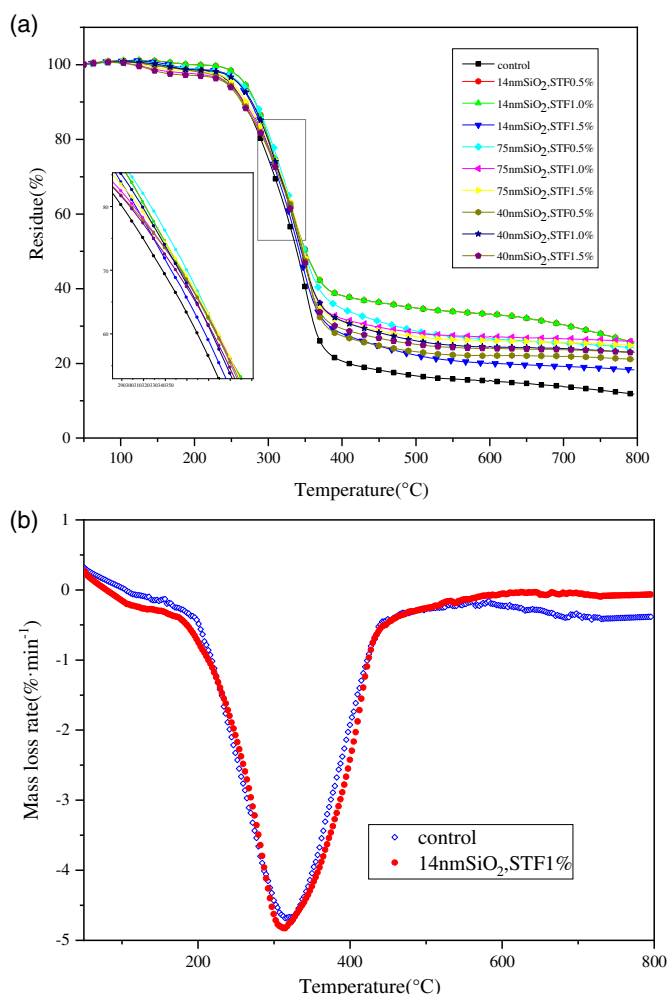


Figure 8. (a) TGA curves of rigid PU foam composites as related to the content of STF and the particle size of SiO₂; (b) DTG curves of rigid PU foam composites made with 1.0 wt % STF containing 14 nm SiO₂. [Color figure can be viewed at wileyonlinelibrary.com]

increasing STF. For the composites made with 1.5 wt % STF that contains 40 nm SiO₂, the coefficient of thermal conductivity is greater than that of the control group, 0.428. In addition, despite the content of STF, the composites containing 75 nm SiO₂ consistently have a great coefficient of thermal conductivity. The results are ascribed to the alcohols of STF. The addition of STF is the

equivalent of adding more foaming agent A, which increases the number of bubbles while decreasing their relative volume during the foaming process. An excessive SiO₂ particle size prevents an even dispersion of STF, but instead engenders agglomeration. The cell morphology is uneven and destroyed, and the restrained air in the interior increases the coefficient of thermal conductivity and decreases the heat-insulating property of the composites.^{29,30}

Effect of Content of STF and Particle Size of SiO₂ on Coefficient of Acoustic Absorption of Rigid STF/PU Foam Composites

Figure 7 shows the relationship between rigid STF/PU foam composites and the content of STF in terms of coefficient of acoustic absorption. The air chamber sizes are 0, 1, and 2 cm, as seen in Figure 7(a–c). Figure 7(d) shows the coefficient of acoustic absorption of the composites that are made with 1 wt % STF containing 14 nm SiO₂. This study proposes to produce sound-absorbent materials against noise at low frequencies. Regardless of the air chamber size, the coefficient of acoustic absorption exhibits the lowest characteristic peak when the composites are made with 1 wt % STF containing 14 nm SiO₂. When the size of the air chamber is 0 mm, the composites made with 1 wt % STF containing 14 nm SiO₂ have the highest sound absorption peak at 3060 Hz, and the composites made with 1.5 wt % STF containing 14 nm SiO₂ exhibit the second-highest sound absorption peak at 3640 Hz, which indicates that the former has the optimal acoustic-absorbing effect at low frequencies. In particular, Figure 7(d) shows that when the size of the air chamber is 2 cm, the composites have the maximum coefficient of acoustic absorption of 0.841 at 2508 Hz, where a relatively higher peak value can be observed. Figure 7(b,c) shows that for SiO₂ particle sizes of 40 nm and 75 nm, the composites that are made with 0.5 wt % STF have the maximum coefficient of acoustic absorption, which is 200–600 Hz higher than the maximum coefficient of acoustic absorption of composites made with 1.5 wt % STF containing 14 nm SiO₂. Increasing the content of STF changes the coefficient of acoustic absorption of the composites to different levels. In particular, a small particle size of SiO₂ and a content of STF of 0.5–1 wt % help to create a greater acoustic-absorbing effect in the composites. Small-sized SiO₂ granules only slightly accelerate the foaming process, whereas excessive-sized SiO₂ granules damage the internal structure of the composites, sabotaging the coefficient of acoustic absorption.²⁴ Specifically, the optimal sound absorption occurs when composites are made with 1.0 wt % STF containing 14 nm SiO₂.

Thermogravimetric Analysis

Figure 8 shows the TGA and differential thermal analysis curves of the rigid STF/PU foam composites as related to the content of STF and the particle size of SiO₂. The related data of TGA are listed in Table II, where $T_{5wt\%}$ is the temperature of initial degradation and T_{peak} is the temperature of shortest degradation. Figure 8 and Table II show that the pure rigid PU foam without STF has a temperature of initial degradation of 241.4 °C, and after the TG test conducted at 800 °C, the residues make up 22.94 wt % of the total mass. The rigid STF/PU foam composites have a higher temperature of initial degradation, which is due to the addition of different contents of STF containing SiO₂ at

Table II. TG Results of the Rigid PU Foam Composites

Sample	$T_{5wt\%}$ (°C)	$T_{50wt\%}$ (°C)	T_{peak} (°C)	Residue at 800 °C(wt %)
Control (without STF)	241.4	345.6	346.8	22.94
14 nm SiO ₂ /STF 0.5 wt %	247.8	338.3	347.6	11.77
14 nm SiO ₂ /STF 1.0 wt %	266.9	351.2	330.0	25.44
14 nm SiO ₂ /STF 1.5 wt %	264.1	340.4	337.3	16.92
75 nm SiO ₂ /STF 0.5 wt %	258.8	341.8	340.2	18.26
75 nm SiO ₂ /STF 1.0 wt %	261.6	349.0	334.1	24.23
75 nm SiO ₂ /STF 1.5 wt %	244.1	347.3	346.8	25.92
40 nm SiO ₂ /STF 0.5 wt %	250.5	347.5	346.3	24.77
40 nm SiO ₂ /STF 1.0 wt %	244.4	346.4	348.9	21.12
40 nm SiO ₂ /STF 1.5 wt %	258.7	345.1	339.0	22.92

different particle sizes. This result indicates that the addition of STF has a positive influence on the thermal stability of the rigid STF/PU foam composites. Specifically, the composites that consist of 1.0 wt % STF containing 14 nm SiO₂ have the highest decomposition temperature and the highest temperature to yield a weight-loss ratio of 50 wt %. The corresponding temperature of shortest decomposition is increase, and the remaining mass also makes up a greater ratio of the original mass, at 25.44 wt %. The addition of STF results in an increase in residual charcoal, which is probably due to the physical blocking effect of SiO₂.^{31,32} As a result, the optimal thermal stability occurs when the composites are made with 1.0 wt % STF containing 14 nm SiO₂.

CONCLUSIONS

Polyurethane foam has intrinsically low thermal conductivity and good thermal insulation. The thermal insulation property of the rigid PU foam composites is inversely proportional to the content of STF. Namely, a greater content of STF and a greater particle size of SiO₂ are beneficial for the coefficient of thermal conductivity but detrimental to the thermal insulation. Using STF as an additive changes the internal structure and density of the foam. The mechanical properties are also changed, and the composites have a greater compressive property and good acoustic-absorbing effect. The nanograde SiO₂ in the STF is the major cause of the change in the structure of the composites. Moreover, different particle sizes of SiO₂ and contents of STF have a drastic influence on the structure and properties of the composites, which can be demonstrated in opposite trends. When STF consists of 14 or 75 nm SiO₂, the greater the STF, the higher the compressive strength, which is the opposite of the case for STF containing 40 nm SiO₂. The cell morphology is severely damaged when the composites are composed of more STF containing 75 nm SiO₂. Although the composites that are composed of 0.5 wt % STF containing 75 nm SiO₂ have the highest coefficient of sound absorption, those that are composed of 1.0 wt % STF containing 14 nm SiO₂ have the second highest coefficient of sound absorption at the lowest frequency of 2500 Hz, which is 200–500 Hz lower than that of other groups, indicating a good absorption at low frequencies. The addition of STF increases the temperature of initial decomposition by 4 to 24 °C and changes the density of the composites. Therefore, it helps to slightly improve the thermal stability and changes the bending, compression, and mechanical properties. The internal structure of the composite is also dependent on the particle size of SiO₂. However, an excessive content of STF or an excessive particle size of SiO₂ adversely affects the internal structure and the required properties of the composites. In sum, the optimal combination is 1.0 wt % STF and 14 nm SiO₂, giving rigid STF/PU foam composites with good mechanical properties, acoustic absorption, thermal insulation, and thermal stability.

ACKNOWLEDGMENTS

The authors gratefully acknowledge the financial support provided by the National Natural Science Foundation of China (grants 51503145 and 11702187), the Natural Science Foundation of Tianjin (grant 18JCQNJC03400), and the Natural Science Foundation of Fujian (2018J01504 and 2018J01505). This study is

also supported by the Open Project Program of Fujian Key Laboratory of Novel Functional Fibers and Materials (Minjiang University), China (FKLTfM1718 and FKLTfM1722), the Opening Project of Green Dyeing and Finishing Engineering Research Center of Fujian University (2017001A, 2017001B, 2017002B, 2017004B), and the Program for Innovative Research Team in University of Tianjin (TD13-5043).

REFERENCES

1. Sun, L. L.; Xiong, D. S.; Xu, C. Y. *J. Appl. Polym. Sci.* **2013**, 129(4), 1922.
2. Lee, Y. S.; Wetzel, E. D.; Wagner, N. J. *China Pers. Protect. Equip.* **2016**, 38(13), 2825.
3. Lin, J. H.; Chuang, Y. C.; Li, T. T. *Materials*. **2016**, 9(12), 1000.
4. Dourbash, A.; Buratti, C.; Belloni, E.; Motahari, S. *J. Appl. Polym. Sci.* **2016**, 134, 44521. <https://doi.org/10.1002/app.44521>.
5. Gama, N.; Rui, S.; Carvalho, A. P. O.; Ferreira, A.; Barros-Timmons, A. *Polym. Test.* **2017**, 62(62), 13.
6. Damian, R. M.; Tiuc, A. E.; Vermeşan, H.; Gabor, T.; Vasile, O. *Energy Procedia*. **2016**, 85, 559.
7. Vasanthakumari, R. *Int. J. Sci. Eng. Res.* **2013**, 4, 301.
8. Verdolotti, L.; Maio, E. D.; Lavorgna, M.; Iannace, S. *J. Mater. Sci.* **2012**, 47(19), 6948.
9. Michałowski, S.; Hebda, E.; Pielichowski, K. *J. Therm. Anal. Calorim.* **2017**, 130(1), 155.
10. Zheng, Z.; Wang, L.; Li, D.; Huang, Z.; Adhikari, B.; Chen, X. D. *Int. J. Food Eng.* **2016**, 12(9), 911. <https://doi.org/10.1515/ijfe-2016-0166>.
11. Kausar, A.; Siddiq, M. *Int. J. Polym. Anal. Charact.* **2016**, 21(5), 436.
12. Xu, Z.; Tang, X.; Zheng, J. J. *Macromol. Sci., Part D: Rev. Polym. Process.* **2008**, 47(11), 1136.
13. Gürgen, S.; Kuşhan, M. C.; Li, W. *Korea-Australia Rheol. J.* **2016**, 28(2), 121.
14. Czupryński, B.; Paciorek-Sadowska, J.; Liszkowska, J. *J. Appl. Polym. Sci.* **2006**, 100(3), 2020.
15. Xu, W.; Wang, G. *J. Appl. Polym. Sci.* **2015**, 132, 42298. <https://doi.org/10.1002/app.42298>.
16. Septevari, A. A.; Evans, D. A. C.; Annamalai, P. K.; Martin, D. J. *Ind. Crops Prod.* **2017**, 107, 114.
17. Biedermann, A.; Kudoke, C.; Merten, A.; Minogue, E.; Rotermund, U.; Seifert, H. *High Temp. - High Pressures*. **2001**, 33(6), 699.
18. Marsavina, L.; Linul, E.; Voiconi, T.; Sadowski, T. *Polym. Test.* **2013**, 32(4), 673.
19. Verdolotti, L.; Maio, E. D.; Lavorgna, M.; Iannace, S. *J. Mater. Sci.* **2012**, 47(19), 6948.
20. Li, T. T.; Lou, C. W.; Hsu, Y. H.; Lin, J. H. *J. Appl. Polym. Sci.* **2014**, 131(13), 53.
21. Wang, Y.; Zhu, Y.; Yaqin, F. U. *Nano*. **2014**, 09(08), 1450100.

22. Hejna, A.; Kirpluks, M.; Kosmela, P.; Cabulis, U.; Haponiuk, J.; Piszczyk, Ł. *Ind. Crops Prod.* **2017**, 95, 113.
23. Peng, H.; Wang, X.; Li, T. T.; Huang, S. Y.; Wu, L.; Lou, C. W. *J. Sandwich Struct. Mater.* **2018**. <https://doi.org/10.1177/109963621875532>.
24. Li, T. T.; Chuang, Y. C.; Huang, C. H.; Lou, C. W.; Lin, J. H. *Fibers Polym.* **2015**, 16(3), 691.
25. Thirumal, M.; Khastgir, D.; Singha, N. K.; Manjunath, B. S.; Naik, Y. P. *Cell. Polym.* **2007**, 26(4), 245.
26. Kim, M. W.; Kwon, S. H. *eXPRESS Polym. Lett.* **2017**, 11(5), 374.
27. Cha, G. C.; Song, J. S.; Lee, S. M.; Mu, S. M. *Polymer Korea.* **2010**, 34(1), 8.
28. Mohamed, M.; Hussein, R.; Abutunis, A.; Huo, Z.; Chandrashekhara, K.; Sneed, L. H. *J. Sandwich Struct. Mater.* **2016**, 18(6), 769. <https://doi.org/10.1177/1099636215626597>.
29. Nazeran, N.; Moghaddas, J. *J. Non-Cryst. Solids.* **2017**, 461, 1.
30. Zhao, C.; Yan, Y.; Hu, Z.; Li, L.; Fan, X. *Constr. Build. Mater.* **2015**, 93, 309.
31. Praveen, T. A.; Rajan, J. S.; Sailaja, R. R. N. *Compos. Interfaces.* **2016**, 24(2), 215.
32. Liang, S.; Zhu, Y.; Wang, H.; Wu, T.; Tian, C.; Wang, J. *I&EC Res.* **2016**, 55(10), 2721.